SCIENTIFIC REPORTS
nature research

OPEN

CO_2 separation using composites consisting of 1-butyl-3-methylimidazolium tetrafluoroborate/CdO/1-aminopyridinium iodide

Hyun Young Kim[1] & Sang Wook Kang[1,2*]

1-Aminopyridinium iodide (iodine salt) was used in CO_2 separation composites consisting of CdO and 1-butyl-3-methylimidazolium tetrafluoroborate ($BMIM^+BF_4^-$). Using iodine salt, the separation performance was largely improved. The CO_2/N_2 selectivity was 64.6 and the permeance of CO_2 gas was 22.6 GPU, which was about twice that of $BMIM^+BF_4^-$/CdO composites without addition of iodine salt. These results were due to the both effect of iodine salt on the transport of the N_2 molecules by the cyclic ring compound and the promoting transport of CO_2 molecules by the amine groups. Moreover, the oxide layer on the surface of the CdO could enhance the CO_2 solubility, resulting in the enhancement of separation performance. The mechanical and chemical properties were measured using SEM, Raman, TGA and FT-IR. The cross-section of coated membranes was confirmed by SEM. The coordinative interactions of iodine salts with $BMIM^+BF_4^-$/CdO composite were observed by Raman.

Most of the natural gas produced worldwide includes carbon dioxide. Carbon dioxide in nature gas occupies 70% of the total volume of gas[1].

Unfortunately, carbon dioxide could cause corrosion of pipe lines in purification process and reduce the efficiency of natural gas[1,2]. Thus, separating and removing carbon dioxide from natural gas streams and flue gases have been major concern recently, since it could prevent pipeline corrosion and reduce global warming effects[3–6]. There were conventional carbon dioxide separation technologies to have been commonly used, such as carbon capture and storage (CCS) technology, solid adsorbent, adsorption and stripping using aqueous amine as liquid[7–9]. However, these existing technologies were economically costly and have the disadvantage of operating on a large scale[10]. On the other hand, for the case of membrane technology, it complements these disadvantages since it has many advantages such as being economically efficient, small scale operation, and being environmentally friendly[11–13].

Polymer-based membranes, especially with ether group in their chains, have contributed to strong coordination between CO and oxygen atoms of the polymer[14–17]. This strong coordination could enhance solubility of CO_2 molecules, resulting in the enhancement of CO_2/airy gas selectivity[18]. For example, Liu *et al.* arranged poly(ether block amide)/polysulfone (PEBA/Psf) composite hollow fiber membrane. That membrane achieved a CO_2 permeability up to 260 Barrer (1 Barrer $= 7.5 \times 10^{-15} m^3$ (STP)) $m/m^2 s$ K Pa) and 40–51.5 selectivity of CO_2/N_2[19]. However, since poly(ethylene oxide) (PEO) has a relatively large number of ether group, its mechanical properties were relatively weak even though it has high crystallinity.

For ionic liquid (IL)-based membranes, it has various advantages such as thermally stable and had long- term stability under pressurized conditions. Using these advantages, many researches on various gas separation membranes based on ILs have been reported[20–22]. For example, membrane consisting of 1-hexyl-3-methylimidazolium nitrate ($HmimNO_3$)/Cu nanoparticles (CuNPs) showed a selectivity of 6.2 for CO_2/CH_4 and 7.4 for CO_2/N_2 selectivity[23].

[1]Department of Chemistry, Sangmyung University, Seoul, 03016, Republic of Korea. [2]Department of Chemistry and Energy Engineering, Sangmyung University, Seoul, 03016, Republic of Korea. *email: swkang@smu.ac.kr

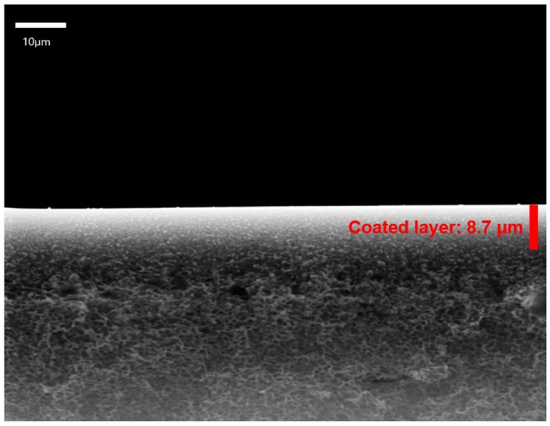

Figure 1. Scanning electron microscopy (SEM): $BMIM^+BF_4^-$/CdO/iodine salt composite membrane.

In our previous study, we have studied the CO_2 permeance and CO_2/N_2 selectivity by preparing membranes by adding various metal oxides to ionic liquids. For example, for the $BMIMBF_4$/ZnO composite membrane, the CO_2 permeance was 101 GPU and the CO_2/N_2 selectivity was 42.1[24]. The ZnO oxide layer has a strong affinity for CO_2 and has been shown to influence the increase in solubility of CO_2. The $BMIMBF_4$/CdO composite membrane had CO_2/N_2 selectivity of 32.5 and a CO_2 permeance of 57.1 GPU[25]. As a result, when the metal oxide was introduced, the oxide layer could improve the CO_2 solubility, which has influenced the CO_2 transport by free ions in the ionic liquid.

In this study, $BMIM^+BF_4^-$/CdO composite membrane was used with an iodine salt containing amine group in metal oxide doped membrane. For these membranes, it was expected that the amine group in iodine salt will interact with CO_2 molecules for solubility enhancement. Furthermore, the CdO nanoparticles have strong affinity for CO_2 capable of enhancing the transport. It was also thought that the synergistic influence of the cyclic ring effect in iodine salt plays a role as barriers for N_2 transport, resulting in the increase of CO_2/N_2 selectivity.

Results and Discussion

SEM images analysis. As shown in Fig. 1, the morphology was examined by SEM and used to investigate the average thickness of the coating solution on the polysulfone microporous support. The average pore size of neat polysulfone was 0.1 μm and pore of surface state was also observed as microporous structure. SEM image showed that the polysulfone support was similar to the sponge like structure and the thickness of selective layer was about 8.7 μm.

Previous studies have shown that the CO_2/N_2 selectivity in the 1/0.007 in the composite membrane of $BMIM^+BF_4^-$/CdO on polymer support with finger-like structure was 32.5[25]. In this study, the shape of the cross-section of the polysulfone support was sponge like structure.

TEM images analysis. To investigate the CdO nanoparticles in $BMIM^+BF_4^-$/CdO/iodine salt composite, TEM was observed as shown in Fig. 2. TEM image showed that the average size of generated CdO nanoparticles were ranged from 100 to 200 nm and the aggregation phenomena was observed.

Separation performance. Figure 3 showed the separation of CO_2/N_2 using a $BMIM^+BF_4^-$ ionic liquid containing CdO particles and iodine salt. The weight ratio of $BMIM^+BF_4^-$/CdO was fixed at 1:0.007 and membranes with increasing mole ratio of iodine salt were tested at room temperature using a single gas (CO_2 and N_2). These experiments were tested three times and the single gas permeances measured for CO_2 and N_2 were described in Fig. 3(a). As the mole ratio of iodine salt increased, the permeance of CO_2 increased to 0.05 mole ratio of salts and decreased above that ratio due to the aggregation phenomena of iodine in composite. These aggregation phenomena of iodine salts prevented the gas molecules from being transported through membrane, diminishing the permeance. Thus, CO_2 permeance decreased with increasing iodine salt to 0.05 mole ratio of salts. Thus, the best separation performance was observed at 0.05 mole ratio of iodine salts as shown in Fig. 3(b).

The single gas permeance and selectivity of the composite membranes: 1/0.007 $BMIM^+BF_4^-$/CdO and 1/0.007/0.05 $BMIM^+BF_4^-$/CdO/iodine salt membranes were compared as shown in Table 1. Table 1 indicated that $BMIM^+BF_4^-$/CdO composite membranes showed the CO_2 permeance of 22.9 GPU and the selectivity of 17.6 (CO_2/N_2) while the CO_2 permeance of 22.6 GPU and the selectivity of 64.6 for $BMIM^+BF_4^-$/CdO/iodine salt composite membranes. These results were attributable to that the iodine salt acts as a hindrance to the moving of gas molecules, resulting in the decrease in overall permeance ('barrier effect'). However, the transport of CO_2 could be accelerated by the amine group of iodine salt. In addition, the interaction between the oxide layer formed from the dissociated CdO nanoparticles and the CO_2 molecule also could improve the solubility of CO_2.

Raman analysis. Raman was measured to investigate the interaction of iodine salt molecule in $BMIM^+BF_4^-$/CdO composite. The Raman spectrum $BMIM^+BF_4^-$/CdO (1/0.007) was described in Fig. 4(a), and the addition of 0.05 mol of iodine salt was shown in Fig. 4(b). The three different ionic species for various BF_4^- states such as ionic aggregates, ion pairs, and free ions were observed at 777, 770, and 765 cm^{-1}, respectively[26]. Table 2

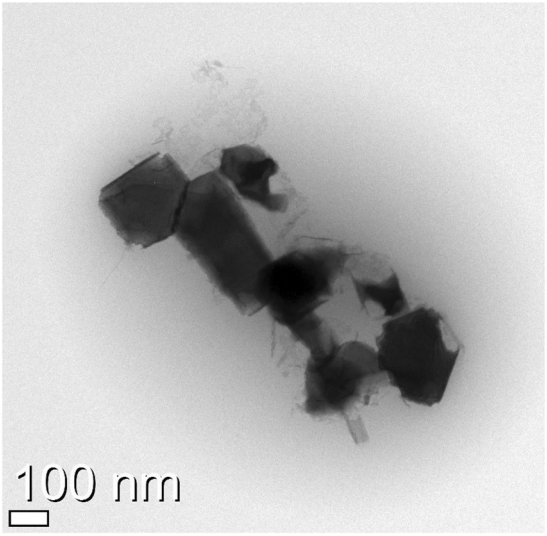

Figure 2. Transmission electron microscopy (TEM) image of CdO particles in $BMIM^+BF_4^-$/CdO/iodine salt composite.

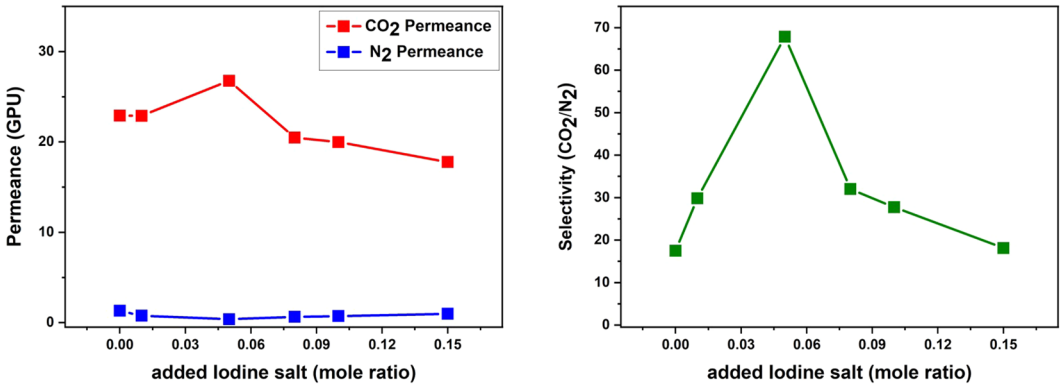

Figure 3. Separation performance of the $BMIM^+BF_4^-$/CdO/iodine salt composite membranes: (**a**) single gas permeance and (**b**) CO_2/N_2 selectivity.

	CO_2 Permeance (GPU)	N_2 Permeance (GPU)	Selectivity (CO_2/N_2)
1/0.007 $BMIM^+BF_4^-$/CdO [finger-like]	57.1	1.8	32.5
1/0.007 $BMIM^+BF_4^-$/CdO [sponge-like]	22.9	1.3	17.6
1/0.007/0.05 $BMIM^+BF_4^-$/CdO/iodine salt [sponge-like]	22.6	0.35	64.6

Table 1. Single gas permeance and selectivity of the composite membranes: 1/0.007 $BMIM^+BF_4^-$/CdO and 1/0.007/0.05 $BMIM^+BF_4^-$/CdO/iodine salt membranes.

compared the deconvolutions of $BMIM^+BF_4^-$/CdO (1/0.007) and $BMIM^+BF_4^-$/CdO/iodine salt (1/0.007/0.05) for each area of BF_4^- species. In the case of $BMIM^+BF_4^-$/CdO/iodine salt, the region of free ions was extended from 35% to 45.7%. These results suggested that new binding of $BMIM^+$ and iodine salt of $BMIM^+BF_4^-$/CdO weakened the interaction between $BMIM^+$ and BF_4^-, leading to the increase in free ions of BF_4^-.

TGA analysis. The TGA of Fig. 5 was measured at room temperature up to 600 °C. In particular, the thermal stability of the $BMIM^+BF_4^-$/CdO composite and $BMIM^+BF_4^-$/CdO/iodine salt composites was compared using a TGA analysis. In the case of $BMIM^+BF_4^-$/CdO composite, the weight loss occurred at 390 ~ 530 °C while $BMIM^+BF_4^-$/CdO/iodine salt composite lost the weight at 200 ~ 500 °C. The overall graph showed that when CdO and iodine salt were added, the stability of $BMIM^+BF_4^-$ was gradually reduced. When CdO was added, the CdO particles were well dispersed in $BMIM^+BF_4^-$, resulting in that the interactions between $BMIM^+BF_4^-$ and

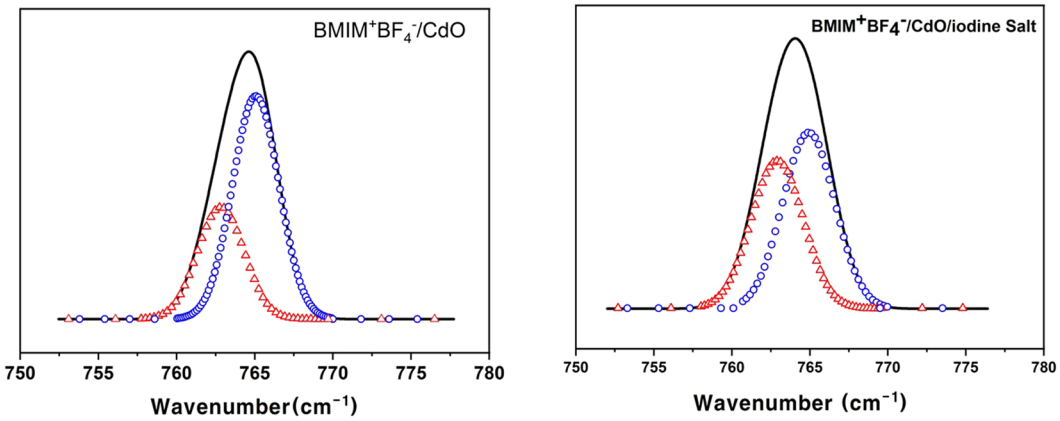

Figure 4. Raman spectra of (**a**) 1/0.007 $BMIM^+BF_4^-$/CdO and (**b**) 1/0.007/0.05 $BMIM^+BF_4^-$/CdO/iodine salt composite. Circles and triangles indicate free ion and ion pairs.

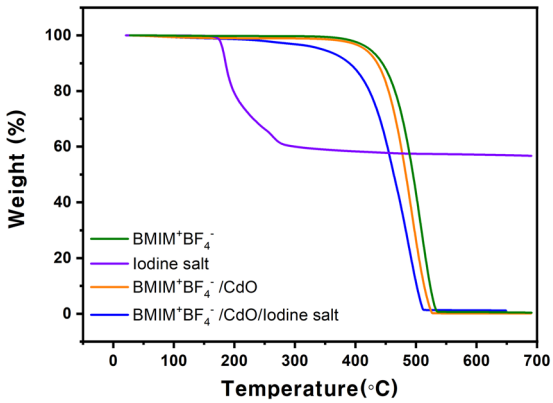

Figure 5. TGA graph of $BMIM^+BF_4^-$/CdO (orange), neat $BMIM^+BF_4^-$ (green), $BMIM^+BF_4^-$/CdO/iodine salt (blue) and neat iodine salt (purple).

	Free ions (%)	Ion pair (%)
1/0.007 $BMIM^+BF_4^-$/CdO	35	65
1/0.007/0.05 $BMIM^+BF_4^-$/CdO/iodine salt	45.7	54.3

Table 2. Percentage of every ion species in the 1/0.007 $BMIM^+BF_4^-$/CdO and 1/0.007/0.05 $BMIM^+BF_4^-$/CdO/iodine salt composites.

CdO generated the decrease of thermal stability[25]. Furthermore, the addition of iodine salt caused the iodine salt to be interacted with $BMIM^+BF_4^-$, further reducing thermal stability.

FT-IR analysis. Figure 6 showed the FT-IR spectra for the neat $BMIM^+BF_4^-$ and $BMIM^+BF_4^-$/CdO/iodine salt composites. The C-H stretching band the alkyl group of neat $BMIM^+BF_4^-$ was known to be observed at 2966 cm^{-1}[27]. However, when iodine salt was added to neat $BMIM^+BF_4^-$, it shifted from 2966 to 2962 cm^{-1}, due to the new coordinative interaction.

As shown in Fig. 7, with the new combination of $BMIM^+$ and iodine salt, the existing C-H stretching band was weakened. This also indicated BF_4^- became more free ions when iodine salt was added to $BMIM^+BF_4^-$/CdO in the raman spectra.

Conclusions

We have succeeded in preparing high selective carbon dioxide membranes consisting of $BMIM^+BF_4^-$/CdO/iodine salt composite to facilitate the CO_2 transport for high separation performance. The features and interactions in $BMIM^+BF_4^-$/CdO/iodine salt composites were characterized by SEM, Raman, TGA, and FT-IR. The separation performance of $BMIM^+BF_4^-$/CdO/iodine salt composite membrane was significantly increased compared to $BMIM^+BF_4^-$/CdO composite. When CdO and iodine salt were incorporated into $BMIM^+BF_4^-$, the CO_2/N_2 selectivity was 64.6 and the permeance of CO_2 molecules was 22.6 GPU. These results were due to the both

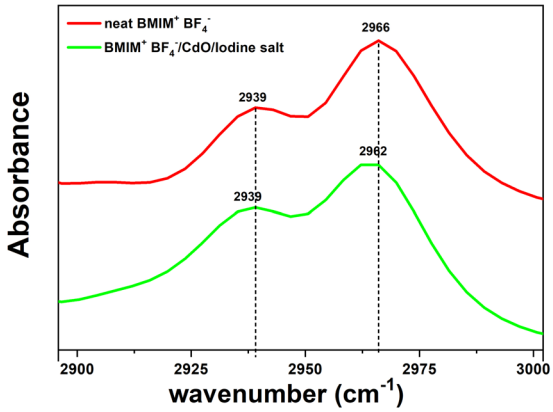

Figure 6. FT-IR spectra of neat $BMIM^+BF_4^-$ and $BMIM^+BF_4^-$/CdO/iodine salt composite.

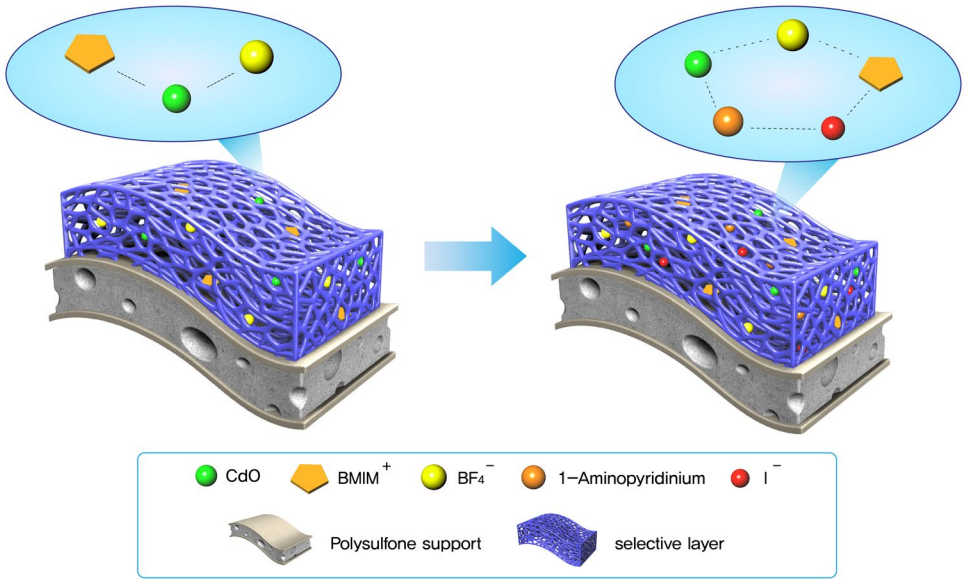

Figure 7. Coordination behavior in 1-butyl-3-methylimidazolium tetrafluoroborate/CdO/1-aminopyridinium iodide composite.

effect of iodine salt on the transport of the N_2 molecules by the cyclic ring compound and the facilitating transport of CO_2 molecules through the amine group.

Methods

Materials. Cadmium oxide (CdO) was supplied from Sigma-Aldrich Chemical Co. 1-Aminopyridinium iodide (Iodine salt, 97%) was supplied from Sigma-Aldrich Chemical Co. 1-Butyl-3-methyl imidazolium tetrafluoroborate ($BMIM^+BF_4^-$) was supplied from Merck KGaA (Darmstadt, Germany). Ethyl alcohol (≥94.0%) was supplied from Daejung Chemicals & Metals. The microporous polysulfone support (average pore size = 0.1 μm) for the enhancement of mechanical property was provided by Toray Chemical Inc., Korea. All the chemicals were used without purification.

Preparation of membranes. The membranes were prepared utilizing $BMIM^+BF_4^-$, cadmium oxide, iodine salt and ethanol. As first step, the cadmium oxide was sonicated to be dispersed in ethanol for 5 minutes. Then, $BMIM^+BF_4^-$ and iodine salt were added to the ethanol mixture with cadmium oxide dispersed. The solution was heated at 85 °C for 24 hours to evaporate the ethanol. Then, solution was coated onto a polysulfone microporous support and cast using a RK control coater (Model K202, Control Coater RK Print-Coat Instruments Ltd., UK). The best performance of $BMIM^+BF_4^-$/CdO/iodine salt was observed at 1/0.007/0.05 (The ratio of $BMIM^+BF_4^-$/CdO was described by weight ratio while $BMIM^+BF_4^-$/iodine salt was mole ratio).

Gas separation experiments. The all gas flow rates represented by gas permeance were determined using a bubble flow meter at the steady-state. Gas flow rates were measured with a mass flow meter at an upstream with

various pressure of psig and atmospheric downstream pressure. The permeances of CO_2 and N_2 were measured in gas permeance units (GPU), where 1 GPU = 1×10^6 cm^3 (STP)/(cm^2·s·cmHg) and the ideal selectivity was defined as CO_2 permeance divided by N_2 permeance.

Characterization. The scanning electron microscope (SEM; JSM – 5600 LV, JEOL) characterized prepared membranes. The transmission electron microscope (TEM; Tecnai F20 G^2–200 KV, FEI) was used to characterize the CdO nanoparticle ranges in composite. The weight loss was collected using a thermogravimetric analysis (TGA; Q50 TA Instrument) of the composite membrane in flowing N_2. Raman spectra of for $BMIM^+BF_4^-$/CdO solution and $BMIM^+BF_4^-$/CdO/iodine salt solution were obtained using a BRUKER RAM II instrument at a resolution of 4 cm^{-1} at room temperature. The IR measurements were used on a VERTEX 70 FT-IR spectrometer; 16–32 scans were done at a resolution of 8 cm^{-1}. A sonifier were used Branson 450 (Branson Ultrasonics Corporation, Danbury CT, USA) with a standard tip.

Received: 16 August 2019; Accepted: 26 October 2019;
Published online: 12 November 2019

References

1. Keller, M. Problems of epidemiology in alcohol problems. *J. Stud. Alcohol* **36**, 1442–1451 (1975).
2. Assink, R. Fouling mechanism of separator membranes for the iron/chromium redox battery, *J. mem. Science* **17**, 205–217 (1984).
3. Lee, D., Ryu, H.-J., Shun, D., Bae, D.-H. & Baek, J.-I. Effect of solid residence time on CO_2 selectivity in a semi-continuous chemical looping combustor. *Korean J. Chem. Eng.* **35**, 1257–1262 (2018).
4. Wang, Y. *et al*. Adsorption of carbon dioxide and water vapor on fly-ash based ETS-10. *Korean J. Chem. Eng.* **35**, 1642–1649 (2018).
5. Rodenas, T. *et al*. Metal–organic framework nanosheets in polymer composite materials for gas separation. *Nature Mater* **14**, 48–55 (2015).
6. Ramezani, R., Mazinani, S. & Di Felice, R. Potential of different additives to improve performance of potassium carbonate for CO_2 absorption. *Korean J. Chem. Eng.* **35**, 2065–2077 (2018).
7. Sevill, M., Ferrero, G. A. & Fuertes, A. B. Beyond KOH activation for the synthesis of superactivated carbons from hydrochar. *Carbon* **114**, 50–58 (2017).
8. Singh, G., Kim, I. Y., Lakhi, K. S., Srivastava, P., Naidu, R. & Vinu, A. Single step synthesis of activated bio-carbons with a high surface area and their excellent CO2 adsorption capacity. *Carbon* **116**, 448–455 (2017).
9. Kumar, S. & Mondal, M. K. Equilibrium solubility of CO_2 in aqueous binary mixture of 2-(diethylamine)ethanol and 1, 6-hexamethyldiamine. *Korean J. Chem. Eng.* **35**, 1335–1340 (2018).
10. Du, N., Park, H. B., Dal-Cin, M. M. & Guiver, M. D. Advances in high permeability polymeric membrane materials for CO_2 separations. *Energy Environ. Sci.* **5**, 7306–7322 (2012).
11. Zhao, C. *et al*. Hybrid membranes of metal–organic molecule nanocages for aromatic/aliphatic hydrocarbon separation by pervaporation. *Chem. Commun.* **50**, 13921–13923 (2014).
12. Trinh, T. T., van Erp, T. S., Bedeaux, D., Kjelstrup, S. & Grande, C. A. A procedure to find thermodynamic equilibrium constants for CO_2 and CH_4 adsorption on activated carbon. *Phys. Chem. Chem. Phys.* **17**, 8223–8230 (2015).
13. Liu, H.-X., Wang, N., Zhao, C., Ji, S. & Li, J.-R. Membrane materials in the pervaporation separation of aromatic/aliphatic hydrocarbon mixtures — A review. *Chinese Journal of Chemical Engineering* **26**, 1–16 (2018).
14. Sánchez-Fuentes, C. *et al*. Interactions between the Ionic Liquid and the ZrO_2 Support in Supported Ionic Liquid Membranes for CO_2 Separation. *Technologies* **4**, 32 (2016).
15. Babucci, M., Akçay, A., Balci, V. & Uzun, A. Thermal Stability Limits of Imidazolium Ionic Liquids Immobilized on Metal-Oxides. *Langmuir* **31**, 9163–9176 (2015).
16. Steinrück, H.-P. *et al*. Surface Science and Model Catalysis with Ionic Liquid-Modified Materials. *Adv. Mater.* **23**, 2571–2587 (2011).
17. Giel, V., Morávková, Z., Peter, J. & Trchová, M. Thermally treated polyaniline/polybenzimidazole blend membranes: Structural changes and gas transport properties. *Journal of Membrane Science* **537**, 315–322 (2017).
18. Yampolskii, Y. Polymeric Gas Separation Membranes. *Macromolecules* **45**, 3298–3311 (2012).
19. Liu, L., Chakma, A. & Feng, X. Preparation of hollow fiber poly(ether block amide)/polysulfone composite membranes for separation of carbon dioxide from nitrogen. *Chemical Engineering Journal* **105**, 43–51 (2004).
20. Yave, W., Car, A., Funari, S. S., Nunes, S. P. & Peinemann, K.-V. CO_2 -Philic Polymer Membrane with Extremely High Separation Performance. *Macromolecules* **43**, 326–333 (2010).
21. Nagel, C., Günther-Schade, K., Fritsch, D., Strunskus, T. & Faupel, F. Free Volume and Transport Properties in Highly Selective Polymer Membranes. *Macromolecules* **35**, 2071–2077 (2002).
22. Vaughn, J. & Koros, W. J. Effect of the Amide Bond Diamine Structure on the CO_2, H_2S, and CH_4 Transport Properties of a Series of Novel 6FDA-Based Polyamide–Imides for Natural Gas Purification. *Macromolecules* **45**, 7036–7049 (2012).
23. Lee, J. H., Chae, I. S., Song, D., Kang, Y. S. & Kang, S. W. Metallic copper incorporated ionic liquids toward maximizing CO_2 separation properties. *Separation and Purification Technology* **112**, 49–53 (2013).
24. Yoon, K. W., Kim, H., Kang, Y. S. & Kang, S. W. 1-Butyl-3-methylimidazolium tetrafluoroborate/zinc oxide composite membrane for high CO_2 separation performance. *Chemical Engineering Journal* **320**, 50–54 (2017).
25. Kim, H., Sohn, H. & Kang, S. W. CO_2 Separation Membranes Consisting of Ionic Liquid/CdO Composites. *j nanosci nanotechnol* **18**, 5817–5821 (2018).
26. Lee, J. H., Hong, J., Kim, J. H., Kang, Y. S. & Kang, S. W. Facilitated CO_2 transport membranes utilizing positively polarized copper nanoparticles. *Chem. Commun.* **48**, 5298 (2012).
27. Cha, S. *et al*. Structures of ionic liquid–water mixtures investigated by IR and NMR spectroscopy. *Phys. Chem. Chem. Phys.* **16**, 9591–9601 (2014).

Acknowledgements

This study was supported by the Basic Science Research Program (2017R1D1A1B03032583) through the National Research Foundation of Korea (NRF), funded by the Ministry of Science, ICT, and Future Planning. This study was also funded by Korea Environment Industry & Technology Institute (KEITI) as "Technology Program for establishing biocide safety management". (RE201805019).

Author contributions

S.W.K. led the project, conducted the data analysis and reviewed the manuscript. H.Y.K. performed the experiments, collected the data and wrote the paper.

Competing interests
The authors declare no competing interests.

Additional information
Correspondence and requests for materials should be addressed to S.W.K.

Reprints and permissions information is available at www.nature.com/reprints.

Publisher's note Springer Nature remains neutral with regard to jurisdictional claims in published maps and institutional affiliations.

Open Access This article is licensed under a Creative Commons Attribution 4.0 International License, which permits use, sharing, adaptation, distribution and reproduction in any medium or format, as long as you give appropriate credit to the original author(s) and the source, provide a link to the Creative Commons license, and indicate if changes were made. The images or other third party material in this article are included in the article's Creative Commons license, unless indicated otherwise in a credit line to the material. If material is not included in the article's Creative Commons license and your intended use is not permitted by statutory regulation or exceeds the permitted use, you will need to obtain permission directly from the copyright holder. To view a copy of this license, visit http://creativecommons.org/licenses/by/4.0/.

© The Author(s) 2019